Metal–Organic Hybrid Interface States of A Ferromagnet/Organic Semiconductor Hybrid Junction as Basis For Engineering Spin Injection in Organic Spintronics

Stefan Lach, Anna Altenhof, Kartick Tarafder, Felix Schmitt, Md. Ehesan Ali, Michael Vogel, Jens Sauther, Peter M. Oppeneer, and Christiane Ziegler*

Electrons in organic semiconductors (OSC) possess remarkably long spin relaxation times. Hybrid spintronic devices that combine OSC with ferromagnetic (FM) substrates are therefore expected to provide a route to devices with improved and new functionalities. A crucial role is played by the FM-OSC interface which governs the spin injection into the OSC. Using spin-resolved photoelectron spectroscopy and ab initio calculations we study here such possible injection channels in metal phthalocyanines (MPc). We report the first direct observation of the successful engineering of different spin-selective hybrid interface states at the Fermi level of a FM-OSC hybrid junction only by changing the central metal atom of a MPc. Our results demonstrate that tailoring the chemical interaction at the FM-OSC interface is a promising way to modify the spin injection channels and thus the spin injection capability.

1. Introduction

A major challenge today is the development of semiconductor-based logical units with magnetic-based data storage units. The focus has turned in the last few years to ferromagnetic-organic semiconductors (FM-OSC) hybrid systems, which are considered to be particularly promising,[1–5] because very long spin-relaxation times were determined in OSC.[1,6–9] However, in spite of these promising features the crucial spin injection from a spin-polarized metallic contact into the OSC is still not understood. In **Figure 1** this problem is illustrated in a pictorial model (without dipole effects).

Dr. S. Lach, A. Altenhof, F. Schmitt, M. Vogel, Dr. J. Sauther, Prof. Ch. Ziegler
Department of Physics and Research Center OPTIMAS
University of Kaiserslautern
Erwin-Schrödinger-Straße 56, D-67663 Kaiserslautern, Germany
E-mail: lach@physik.uni-kl.de
Dr. K. Tarafder, Dr. Md. E. Ali, Prof. P. M. Oppeneer
Department of Physics and Astronomy
Uppsala University
Box 516, S-75120 Uppsala, Sweden
Dr. E. Ali
Center for Theoretical Chemistry
Ruhr-University Bochum
D-44801 Bochum, Germany

DOI: 10.1002/adfm.201102297

For most effective electrical charge injection in a real organic device the injection barrier, i.e. the energy difference Φ_p/Φ_n between the highest occupied/unoccupied molecular orbital HOMO/LUMO and the Fermi level (E_F) must be overcome (Figure 1a). Thus one has to apply a bias voltage of the same magnitude which can shift the HOMO/LUMO to E_F. The dilemma is, that this ohmic-like contact enables charge injection at the interface but not necessarily a spin polarized injection (Figure 1b). The reason for this is the so-called conductance mismatch problem, which was originally developed for inorganic semiconductors in contact with metallic ferromagnets.[10] Because of the much lower conductance (high resistance) of the semiconductor, or, here, the OSC compared to the highly conductive ferromagnetic metal contacts (low resistance) the spin properties of the interface should be dominated by the majority/minority resistance of the OSC itself, as in a pristine non-magnetic OSC the spin-up/down resistances are normally equal. One possibility to solve this dilemma is having a resistance at the interface, e.g., for the minority spin, which is distinctly higher than the resistance of the OSC itself, and a slightly lower resistance for the majority carriers. This can be achieved by inserting an additional tunnelling barrier (inorganic or organic) as a spin selective resistance, acting as a spin filter[5] (Figure 1c). On account of the spin dependent high resistance of such a tunnel barrier, there is a small probability of spin-polarized electrons injected into the OSC at the interface losing their spin information by returning back into the FM. However, the fact that successful spin injection in organic spin valves was reported without using a tunnelling barrier and for only a few millivolts bias voltage,[3] shows that the behavior of OSC at the OSC/FM interface cannot be explained within the conventional model used for inorganic semiconductors. The exceptional nature of OSC molecules and their manifold binding mechanisms obviously complicate the spin selective properties at the OSC/FM interface. Conversely, exactly this manifold of binding mechanisms, not available in pure inorganic devices, opens up possibilities to tailor the spin injection in a novel way. Here we will further develop a promising method based on the molecule specific chemical interaction with a ferromagnetic spin

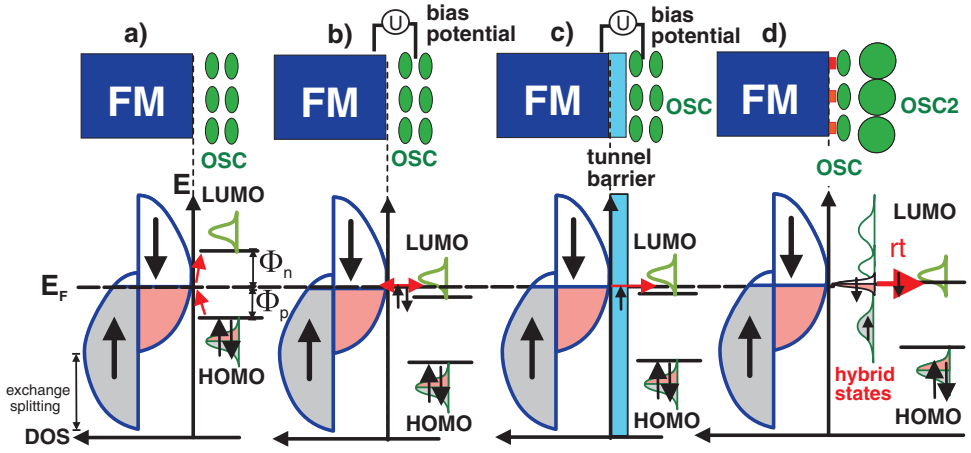

Figure 1. Pictorial model of the energy level alignment and the density of states (DOS) at the FM-OSC monolayer. a) Injection barrier formed at an idealized interface between a spin-polarized (due to exchange splitting) ferromagnetic metal (FM) substrate and an organic semiconductor (OSC) neglecting any chemical interaction and dipole effects: For effective electrical charge injection without any voltage applied, the injection barrier Φ_p/Φ_n for holes/electrons must be overcome because this process is spin-undiscriminating;. b) By applying a bias voltage, an ohmic like behavior of the interface can be achieved. However, due to the conductance mismatch caused by the spin undiscriminating high bulk resistance there is a vanishing spin injection into the OSC. c) Tunneling barrier approach: inserting a highly resistive spin-selective tunnel barrier (light blue) at the FM/OSC interface which acts as a spin filter. d) Hybrid interface states (HIS) approach: DOS modification and spin-split states at E_F induced by chemisorption creates new spin-polarized states at E_F which can couple in a resonant tunnelling process (rt) to a second OSC 2 (big circles) with suitable charge transport levels. Such an interface engineering can conserve the spin polarization, and in combination with a second appropriate organic molecule in the subsequent layers can overcome the conductance mismatch obstacle. The actual formation of such HIS is demonstrated here by our experimental data for the FM-OSC interface with OSC = MPcs.

injection contact recently suggested,[11–15] i.e., the approach of utilizing hybrid interface states (HIS) (Figure 1d). As The HIS are formed from the formerly pure molecular levels and electronic states of the metal by chemical interaction a true hybridization is present. This modification at the interface results in a different density of states (DOS) broadening (depending on the strength of the hybridization) for the individual levels and, importantly, spin splitting. These effects can create spin-dependent channels at E_F in the first monolayer (ML) of the OSC itself, as shown in Figure 1d. Thus the first ML of the OSC behaves as a spin filter. For an optimized spin injection into the subsequent layer of such a FM-OSC device, the second layer has to couple with the HIS in a spin conserving way. A possibility to achieve this could be to choose another OSC with an electron affinity near the work function of the OSC-FM interface. In such case resonant tunneling (rt) could occur which can conserve the spin polarization also in the second and subsequent layers of the organic/metallic device (Figure 1d). Hence, chemically induced HIS offer a strategy to tune spin selectively the spin-polarized DOS at E_F in combination with appropriate molecules used for the second layer/bulk and lays out the opportunity to engineer the spin injection efficiency at the FM-OSC interface.

Metal phthalocyanines are regarded as suitable OSC materials.[2] The potential of MPcs with open shell configuration of the central metal ion in combination with FM substrates was recently shown by two-photon photoemission spectroscopy (2PPE). There, not only a very high spin injection efficiency was determined for hot electrons, but also a spin diffusion length as long as 12.6 ± 3.4 nm.[16] Furthermore, a spin-polarized electronic resonance was recently identified at the center of an also open shell CoPc molecule which originated from an induced ferromagnetic exchange coupling of the CoPc and FM substrate.[17,18] Hence, such MPcs represent prototypical systems on which the spin-selective FM-OSC interface interaction can be studied. Here we have chosen CuPc, CoPc, and FePc with essential differences in the molecular frontier orbitals with respect to their open shell occupation sequence and intrinsic spin configuration.[19–21] All three π-conjugated molecules are p-type semiconductors having the same planar molecular structure and point symmetry (D4h).[22] The central metal ion in FePc has a formal d-occupation of d^6, CoPc of d^7, whereas CuPc has d^9. This difference is expected to govern the MPc's specific electronic behavior at a FM-OSC interface. It also determines the electronic coupling to the second layer which, however, is not discussed in this paper.

As FM substrate we chose Co. The spin-dependent density of states (DOS) around E_F is well known from spin-resolved photoelectron spectroscopy and band calculations.[23,24] By preparing only 20 ML thick Co films on a Cu(001) single crystal a slightly tetragonal compressed face centered cubic structure (fcc) can be prepared.[25] Using short magnetic pulses in situ, the Co surface can be magnetized in-plane along the [110] direction. A combination of experimental spin-resolved and spin-integrated photoemission spectroscopy and computational techniques (DFT+U) was employed to unveil the electronic and chemical properties of the FM-OSC interface.

2. Ultraviolet Photoelectron Spectroscopy (UPS)

Photoelectron spectroscopy is a powerful method to extract general information about the electronic changes at FM-OSC interfaces such as the HIS formation as well as the formation and

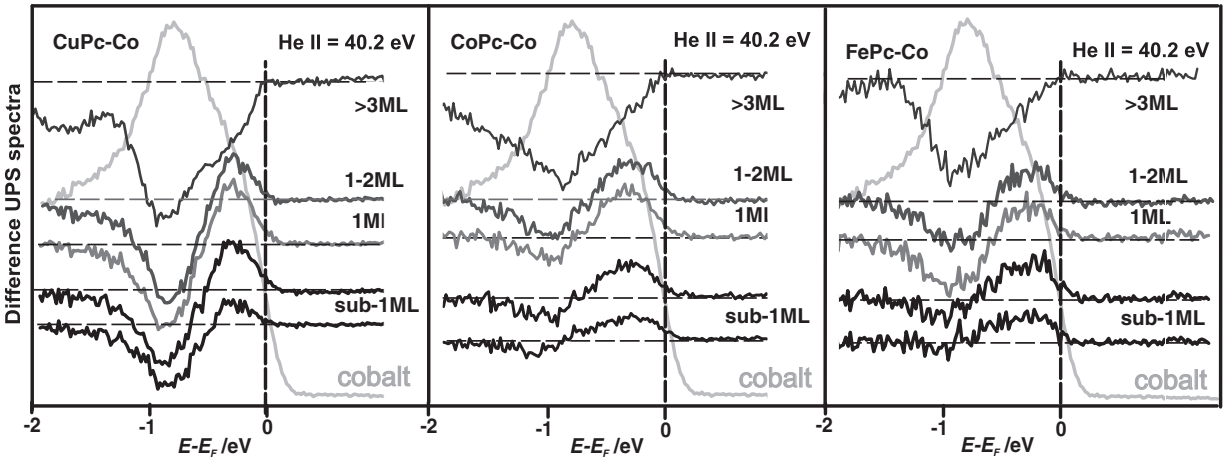

Figure 2. Difference UPS spectra of He II measurements of the CuPc/Co (left), CoPc/Co (center), and FePc/Co interface (right), taken at different film thicknesses going from the submonolayer to the multilayer range. The new hybrid states near the Fermi level E_F have their maximum intensity around 1 ML and vanish for a multilayer coverage. All spectra were normalized at a point 2 eV below E_F. This point was chosen because in this region detailed structures in the DOS of the pristine OSC and the bare cobalt surface (shown in grey color) were not expected.

magnitude of surface dipoles Δ which occur in such a system affecting the SB height at the interface.

Using He I radiation (21.2 eV) enabled us to quickly investigate the development of the initial configuration of the DOS as a function of the OSC coverage at the FM-OSC interface. On account of different photoionization cross-sections for p-orbitals of carbon and nitrogen and d-orbitals of the metal atom[26] and the additional use of He II radiation (40.8 eV) we can estimate the dominating elemental contribution in the experimental DOS.

Referring to the known HOMO structure of the OSC bulk, we detect for all three molecules a comparable maximum size of the surface dipole Δ (0.9 eV, 0.9 eV, and 1.0 eV for CuPc, CoPc, and FePc, respectively) at the bulk-multilayer level with its dipole moment pointing to the molecule. According to the model in Figure 1a an injection barrier Φ_p (Φ_n) of 1.0 eV (0.9 eV) for CuPc, 0.8 eV (1.3 eV) for CoPc, and 0.8 eV (0.8 eV) for FePc creates the unfavorable situation for injecting spin carriers as described in Figure 1a. The same applies for the LUMO. One might infer from these data that all three MPcs are unsuitable candidates for spin-injection from Co. However, as indicated above, it will be shown now, that a chemical reaction between the surface metal atoms and the OSC forming new hybrid states between metal and molecule indeed drastically changes the spin-selective injection channels at E_F of such a FM-OSC interface. The first indication for the existence of HIS is the appearance of additional structures in the experimentally observed DOS at E_F which was recorded by generating difference spectra ($I_{MPc/Co}$–I_{Co}):

As the OSC thickness increases, the emission from the Co substrate typically becomes suppressed and the spectrum continuously changes towards that of the OSC. In our case the decrease of the Co spectrum doesn't change continuously as expected for a simple superposition of the two components spectra OSC and Co. The intensity at the maximum of the pure Co intensity at about 0.9 eV below the Fermi level is rapidly suppressed by the incrementally grown OSC contrary to a much slower decrease for the density directly at the Fermi level. To obtain a more detailed understanding of this behavior, we generated difference spectra ($I_{MPc/Co}$–I_{Co}), shown in **Figure 2**, to identify modifications like gap states induced by the chemical interaction of the OSC with the Co.

For all three MPcs there are differences in the vanishing cobalt part near the Fermi level in the He II spectra indicating a new gap state with a peak maximum around 0.4 eV below E_F. This gap state increases in intensity up to a nominal film thickness of around 1 ML and disappears for larger coverages. In case of FePc the structure is very broad extending to 0.9 eV below E_F. For CuPc the structure is much sharper, i.e., this DOS structure is energetically more localized than in the case of FePc. This is expected for MOs weakly interacting with the Co surface. CoPc takes an intermediate position.

In principle the appearance of such an interface structure could be explained by several models: In case of a physisorption of the MPc molecules on the Co surface by integer charge transfer (ICT), in case of very weak interaction by resonance of the molecular states with the metal continuum states,[27] or in case of chemisorption of the MPcs by a strong chemical interaction forming hybrid interface states between the metal and the OSC. The first two mechanisms could explain the appearance of a new gap state, but none of them causes the molecular level to split energetically into different spin-polarized states. This is much different in case of a chemically induced rehybridization of the Co substrate orbitals and the OSC MOs forming new chemical bonds, i.e., HIS.[28] As we will show below, in case of the MPc/Co interface (M = Cu, Fe, Co) a splitting into different spin-polarized states takes place indicating a strong rehybridization and therefore the formation of spin-polarized HIS.

3. Spin-Polarized Ultraviolet Photoelectron Spectroscopy (SP-UPS)

To unravel the spin character of the HIS, SP-UPS measurements were performed using He I radiation. The main results are shown in **Figure 3**. There is a remarkably different behavior

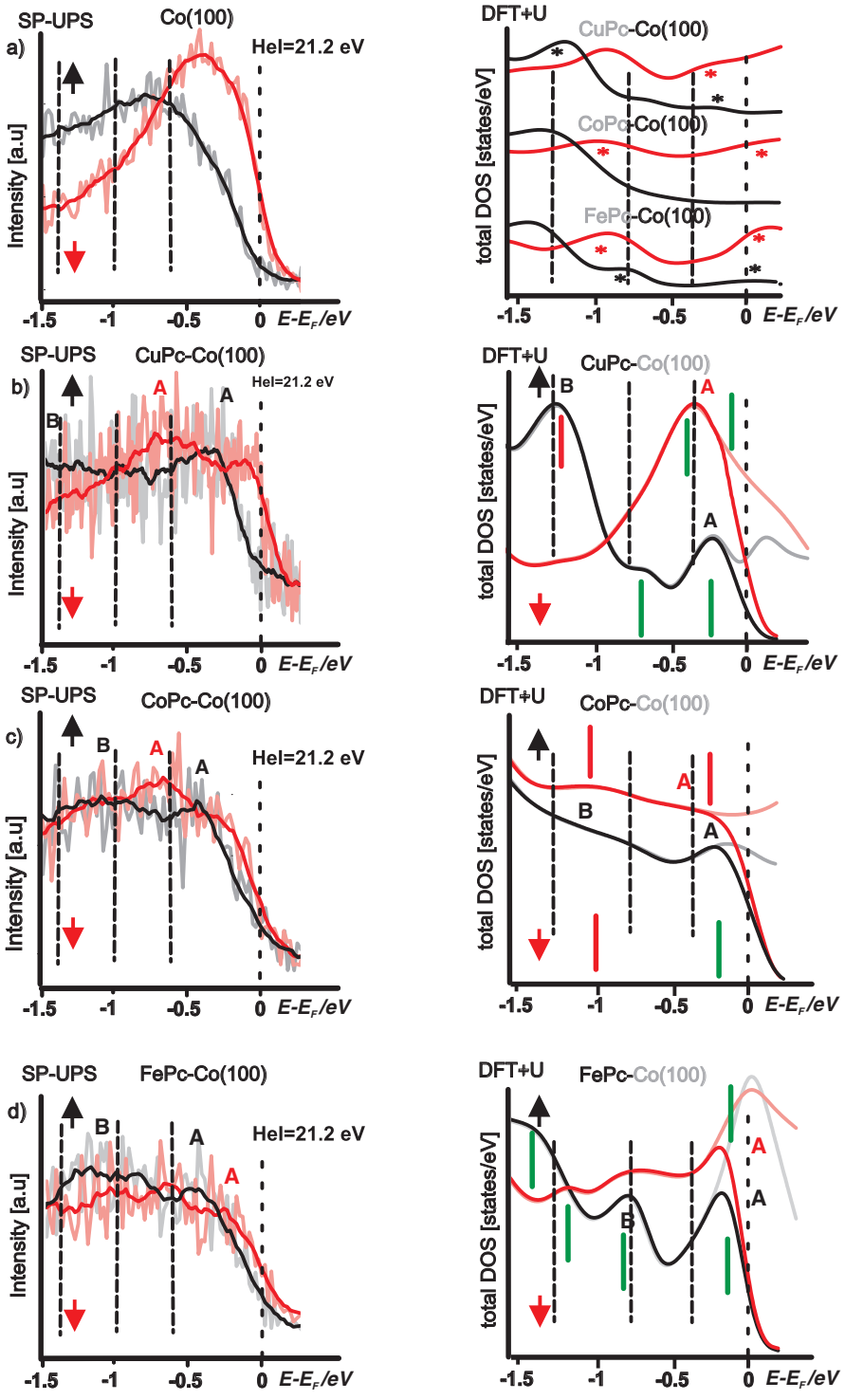

Figure 3. Left: Spin-resolved He I UPS spectra recorded for the spin-up (black) and spin-down (red) DOS of the valence band region around E_F for the pure Co(001) surface a), and a 0.4 nm thin layer of b) CuPc, c) CoPc, and d) FePc on Co(001) in comparison with **Right:** the spin-resolved total density of states (sp-total DOS) for the molecules and the substrate from DFT-GGA+U calculations for chemisorption. For better comparability with the experimental data the energy scale is stretched by a factor of 1.4 and in the region of the Fermi level the total DOS curve was convolved by a Fermi function (original curve shape of the DOS at E_F is shown in translucent color). Comparable substructures in the experimental and the theoretical DOS are indicated by A, B, and spin corresponding colors. Because the contribution of metal or nitrogen DOS alter the experimentally received DOS through differences in their photoemission cross-sections, substructures with mainly metal contribution are highlighted by red bars and substructures dominated by the nitrogen DOS by green bars. All the main substructures (A,B) are in resonance with corresponding DOS structures of the cobalt substrate (indicated by an asterisks and color in a) right).

of the experimental SP-UPS spectra of CuPc, CoPc, and FePc near E_F. The appearance of new substructures especially in the spin-up channel which cannot be assigned to pristine Co rule out that the only modification of the SP-UPS spectra is a simple superposition of the spectra of the substrate and the adsorbed molecules. Because of the hard-to-estimate intensity assigned to the Co in the spectra an advanced analysis by difference spectra, as for the UPS spectra shown above, is not meaningful.

Here only the new substructures will be discussed. As can be seen in Figure 3b, in case of CuPc there is a spin-down (minority spin) dominated DOS localized between E_F and 0.25 eV below, i.e., we see spin-polarization at the Fermi level. There are additional spin-up (majority spin) substructures A at 0.4 eV and B at 1.5 eV, not present in spin-up data of the pure Co surface (Figure 3a). For CoPc (Figure 3c) there is only a weak spin-down polarization at E_F extending down to 0.4 eV. This small polarization is caused by the differences in the slopes of the Fermi distributions of spin-up and spin-down DOS decreasing toward E_F. Additional spin-up substructures around 0.5, and 1.0 and 1.7 eV (the latter not shown here) are found in the experimental spectra which also have no counterpart in the bare Co spectrum. For FePc (Figure 3d) the situation at E_F is very similar to CoPc, i.e., there is effectively no difference in the slopes of the Fermi distribution reductions and therefore only a weak spin-down polarization at E_F. The additional spin-up substructures are A at 0.6 eV and B at 1.1 eV which are also not present in pure Co. This means that for CoPc and FePc the total amount of the polarization at and just below E_F is clearly reduced compared to the native Co substrate. These observations fit with the results of the spin-integrated UPS difference spectra mentioned above and strongly indicate the formation of spin-polarized HIS around E_F for all three MPcs with particularly higher spin down polarization for CuPc directly at E_F in contrast to CoPc and FePc.

Comparing the spin-resolved total DOS from DFT-GGA+U calculations at chemisorption geometry in the right parts of Figure 3 with the experimental data, we note a very good agreement. Observed intensity differences can be explained by the known elemental differences in the photoemission cross-sections using He I radiation.[26] Looking at the calculated DOS at the Fermi level itself, the character of the organic layer has changed from a semiconducting to a metallic behavior especially for FePc with a DOS peak for both spin directions which is cut at its maximum by E_F. The stronger interaction of FePc with Co found in the calculations is reflected by the much broader HIS-DOS also causing a weaker energy separation of the HIS states and therefore spin-polarization as in the case of CuPc with a weaker interaction and less broadened but spin-polarized HIS. The calculated spin-resolved total DOS of CoPc is relatively structureless indicating a strong interaction and rehybridization with the cobalt substrate. For CuPc and CoPc the spin-up total DOS at and just below E_F is dominated by contributions from the nitrogen atoms in contrast to the spin-down total DOS where the central metal contribution is much more pronounced. In case of FePc the distribution between metal and the nitrogen contribution is more balanced. Obviously, of the three studied MPcs, CuPc has an exposed position by its pronounced spin-down polarization at E_F. Looking at the Co substrate signal itself, the spin structure modification through other chemisorption processes, e.g., the reaction with oxygen quickly blurs the spin-structure differences resulting in a strongly vanishing signal intensity with no additional DOS intensity.[24] This also applies for the well-known spin-down polarized surface state found at the bare Co surface.[29] Contrarily, in our data particularly the spin-up DOS near E_F and 1 eV below show strong additional new components. Thus, the spin-related modification of the DOS shown in Figure 3 can only be explained by chemisorption and therefore the formation of differently broadened and spin-split HIS.

To corroborate the chemisorption-induced effect of spin splitting, an additional region between 9 eV to 4 eV below E_F of the valence band was inspected which is structureless in case of the clean native Co surface. As one can see in **Figure 4**, a remarkable band splitting for the spin-up- and down-DOS around 7.5 eV below E_F of $\delta = 0.3$ eV for CuPc, $\delta = 0.1$ eV for CoPc and $\delta = 0.2$ eV for FePc can be identified. Obviously there are also some small differences in the experimental spin-resolved DOS itself which in addition highlight the strong effects near

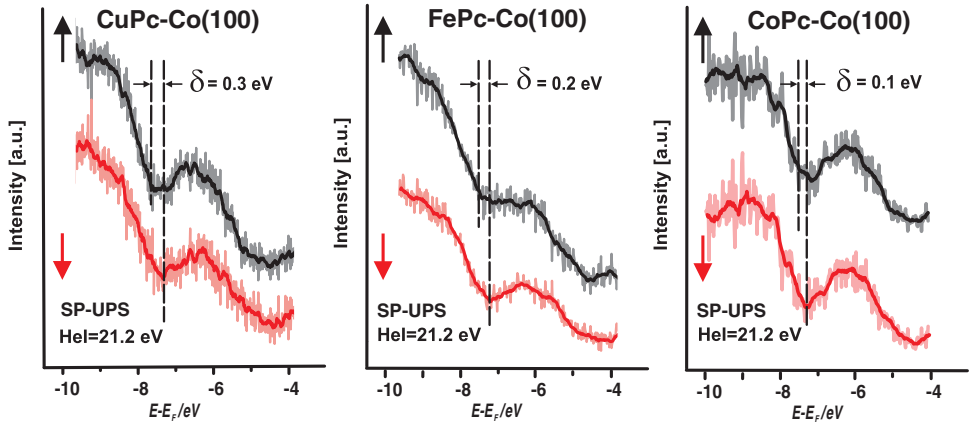

Figure 4. Spin-resolved He I UPS spectra of the valence band region for the 0.4 nm thin layer of CuPc, FePc, and CoPc on Co(001) which was not affected taking residual Co DOS into account, because of the absence of substrate specific DOS in the shown energy region of 9–4 eV below E_F. A remarkable band splitting of $\delta = 0.3$ eV (theoretical $\delta_{theo} = 0.28$ eV) for CuPc, $\delta = 0.2$ eV (theoretical $\delta_{theo} = 0.12$ eV) for FePc, and $\delta = 0.1$ eV (theoretical $\delta_{theo} = 0.08$ eV) for CoPc, with obviously also differences in the experimental spin-resolved DOS itself can be observed.

E_F. Both effects, the band splitting with $\delta_{theo} = 0.28$ eV for CuPc, $\delta_{theo} = 0.08$ eV for CoPc and $\delta_{theo} = 0.12$ eV for FePc and the structural differences are also seen in the calculations (not shown).

Furthermore in this region no structural differences and especially no spin-resolved band splitting can be found in the experimental spectra for a layer thickness of bulk-like behavior. The calculated spin-up vs. spin-down DOS for the single molecule (**Figure 5** below) and the physisorbed state (Supporting Information) indicate no band splitting or spin-dependent structures in this region. However, in the chemisorbed state the experimentally observed splittings as well as the differences in the spin-up and spin-down structure can be recognized in the calculated sp-DOS. Thus the observed experimental modifications strongly indicate the central metal dependent formation of different spin-split HIS induced by the different strengths of the interaction with the Co substrate. In the following we will show by means of the comparison of the calculated spin- and atom- resolved DOS that the differences in the appearance of the molecule specific HIS are mainly induced by the nature of the frontier orbitals of the central metal atom.

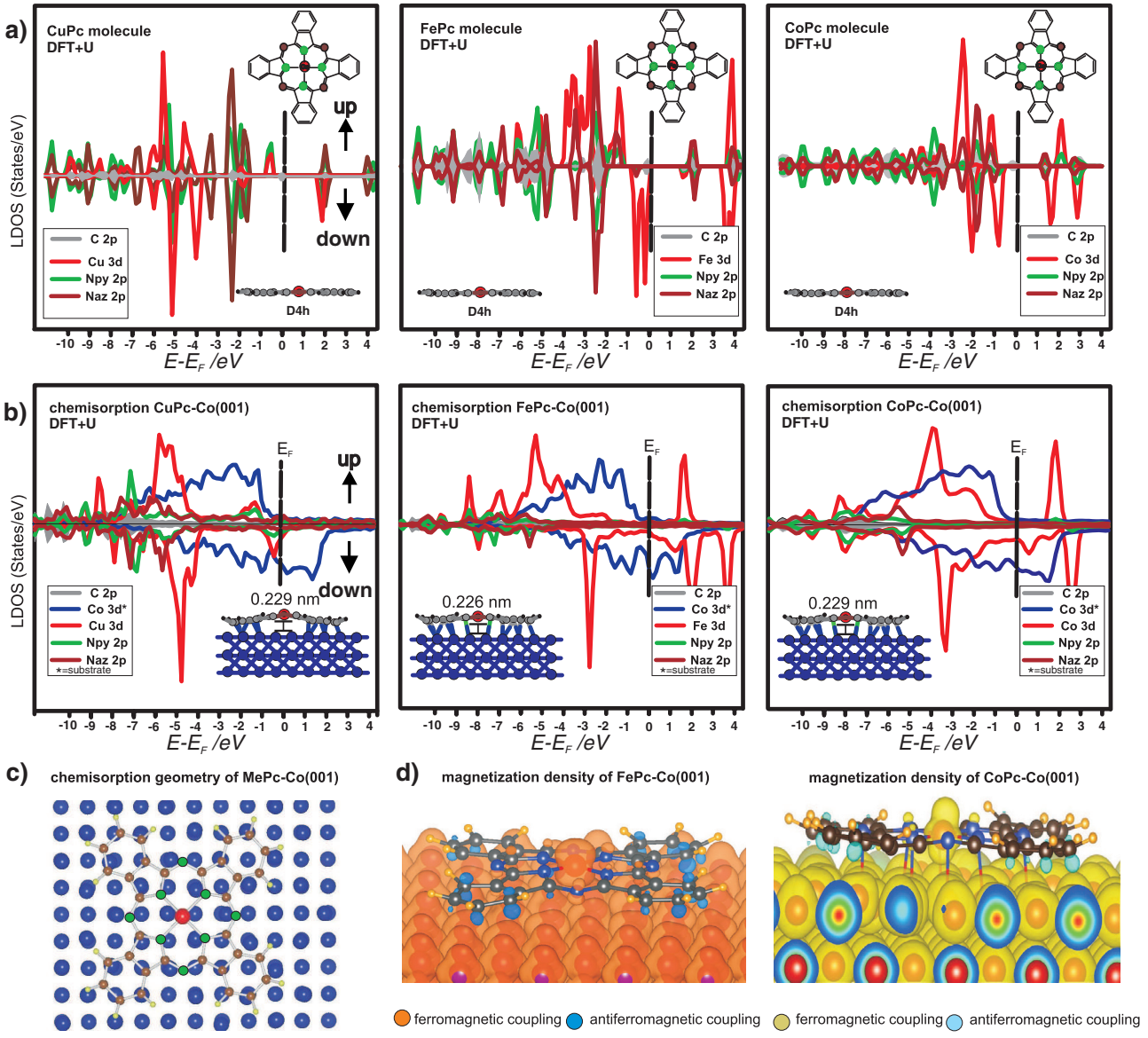

Figure 5. Spin and atom resolved density of states (sp-DOS) calculated with DFT+U, for a) free CuPc, CoPc, and FePc molecules and b) chemisorbed on Co(001) in a bridged position shown in c). The energy scale is stretched for better comparability with the experimental data by a factor of 1.4. The insets show the relaxed adsorption geometry of the molecules on the Co surface. In case of chemisorption (b) the Cu ion bends out of the molecular plane whereas the phenyl rings of CuPc are drawn by up to 0.03 nm toward the surface and away from the plane defined by the Cu ion and the pyrrolic N atoms. For all three molecules the H atoms are pointing away from the surface. The magnetic coupling of FePc and CoPc to Co is shown in (d) where the magnetization density is dominated by the iron and cobalt central atom at the molecular side in an out-of-plane geometry. Note the spin-polarization present on carbon and nitrogen atoms of the phenyl rings, which is created through interaction with the spin-polarized Co-d states of the substrate.

4. Density-Functional Theory-Calculations (DFT+U)

To unveil the origin of the intricate dissimilarities observed between the three FM-OSC interfaces the calculated spin- and atom resolved DOS of free CuPc, CoPc, and FePc molecules as well as for the FM-OSC interface for chemisorbed molecules on the cobalt surface are shown in Figure 5. Chemisorption is computed to be the energetically more stable adsorption state. Furthermore, from calculations of the physisorbed state (Supporting Information (SI)) it could be seen that there are no new HIS observable for CuPc, in contrast to the experimental data, implying a chemisorption interaction occurring at the MPc/Co interface.

As shown in Figure 5c the chemisorption position of the TM ion on the Co surface is a bridging position between two Co atoms. This applies for all three molecules and is accompanied by a further modification of the molecular structure.

In case of CuPc, the Cu atom has now moved out of the molecular plane at an average distance of 0.226 nm from the surface. There is no sign for direct bonds between the Cu or the nitrogen atoms and the Co surface. The obviously distinctive hybridization of the phenyl ring system compared to the nitrogen distorts the molecule causing the hydrogen atoms to point away from the surface and the central copper atom to move slightly out from the formerly planar molecule plane.

This strong interaction is also indicated by the strong broadening of the carbon LDOS in the calculations as well as in the experimental data by an additional shoulder in the C1s core-level spectra found for the low coverage regime (SI) and the absence of similar structures in the N1s-core level. These differences in the interaction of the outer phenyl ring system and the inner center part of the metal organic complex is reflected by the much narrower pyrrolic nitrogen and Cu LDOS localized down to 2 eV below E_F creating the spin off-set for CuPc shown in Figure 3b. The Cu LDOS at E_F is truly a result of rehybridization. The interaction of the Cu atom with the outer phenyl part of the molecule via in-plane oriented MOs with nitrogen contribution results in a massive shift of the formerly unoccupied antibonding Cu state 0.7 eV above E_F (mainly d_{x2-y2} weighted state) to just below E_F. Thus the formerly open shell situation of CuPc with $S = 1/2$ and the single spin located in the b_{1g}-state (the d_{x2-y2} contribution) is now switched to $S = 0$. This is corroborated by the existence of a second monovalent Cu I species centered at 932.9 eV binding energy in the spectra of the Cu $2p_{3/2}$ core level corresponding to a now completely filled 3d orbital in the initial state of the Cu for small coverages as shown in **Figure 6**. This also confirms a vanishing magnetic moment. The in-plane character of the d_{x2-y2} is not favorable for π-type interaction. This additionally explains the deviation of the Cu atom from the molecular plane as described above.

For CoPc the Co(CoPc)-Co(substrate) distance is 0.229 nm. The molecule is not as distorted as in the case of CuPc. The central metal atom is located in the molecular plane such as it is in the free molecule. Nevertheless the hydrogen atoms point away from the surface. Together with a strong distortion of the first Co substrate layer this indicates a strong interaction of the phenyl ring system including the nitrogen atoms and

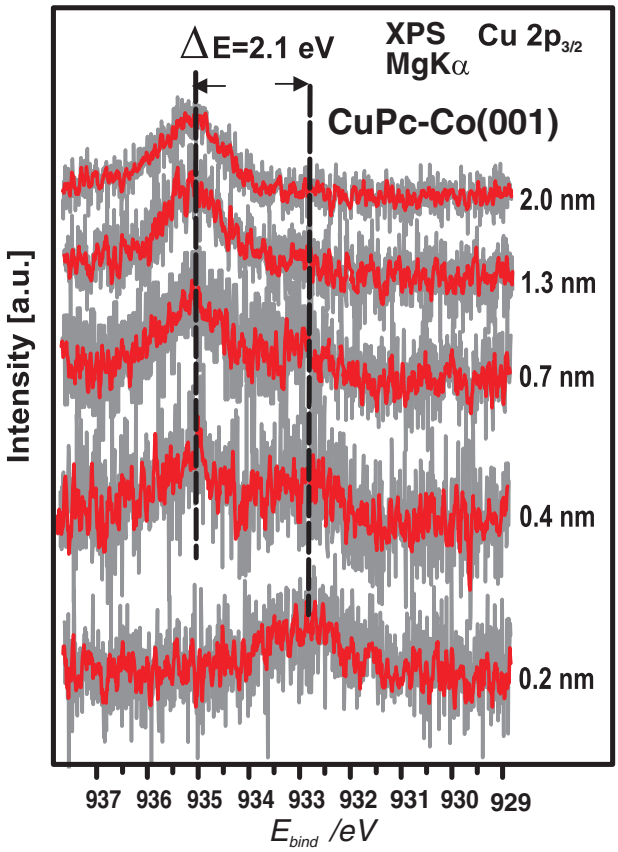

Figure 6. XPS spectra for the Cu $2p_{3/2}$ core levels of CuPc as a function of the layer thickness on Co (001). The peak dominating the spectrum at higher coverage has a binding energy of 935.0 eV and can be attributed to a divalent Cu II state.[32] There is only one peak for the submonolayer coverage (0.2 nm) which is attributed to a monovalent Cu I state, centered at 932.9 eV binding energy and located 2.1 eV below the Cu II state. The copper spectra were normalized to the same height in order to highlight changes in the line shape. For purpose of clearer visibility a 5-point flattening (red) of the raw data (grey) is also shown.

the central metal atom. The reason for this is a strong hybridization of all three out-of-plane d-orbitals (d_{z2}, d_{xz}, d_{yz}) of the central metal Co atom; the former equivalence of d_{xz} and d_{yz} is now lifted. As in FePc (see below) and in contrast to CuPc, the nitrogen atoms of CoPc are partly forming bonds and all of them are deeply involved in the interaction with the cobalt surface. This interaction can be associated with the strongly shifted peak of the CoPc N1s core level ($\Delta E = 1.1$ eV) only observed in XPS at low coverage (SI). Changes in the core level state of the Co central atom could not be observed because of the substrate signal of the Co substrate dominating the core level spectra at low coverage. CoPc couples ferromagnetically to Co (Figure 5d). Whereas in the free CoPc molecule we have S = 1/2 (i.e., μ = 1.004 μ_B being mainly localized in a d_{z2} dominated state), the magnetic moment is now reduced to 0.515 μ_B. The moment on the Co central atom is 0.669 μ_B. There are small negative moments on the carbons and small positive moments on N, in line with a previous report.[17] Concomitant to the interaction of the molecule with the substrate, a strong broadening of the

whole LDOS in the calculations can be seen. The π-interaction of the phenyl ring system is reflected by an additional structure in the C1s core level spectra for the low coverage regime. This is in line with the very strong rehybridization reaction of the three out-of-plane d-orbitals (d_{z2}, d_{xz}, d_{yz}) of the cobalt central atom dominating the electronic interaction of the CoPc/Co interface.

For FePc the Fe-Co distance of 0.224 nm is comparable to the one found for Cu-Co of CuPc on Co. Different from Cu in CuPc (and in part from CoPc), a reduction of the Fe metal atom was not found for FePc, which has a spin $S = 1$ for both, the free and chemisorbed molecule. Furthermore, for FePc the deviation from the ideal molecular plane is much lower than for CuPc and comparable with the one found for CoPc. This indicates a similar role of the phenyl rings for the interaction of FePc with cobalt as in CoPc. The hybridization of the phenyl rings with the Co generates broadening of the carbon LDOS up to E_F. This is also observable by a broadening in the C1s core-level spectra of the FePc-Co interface (suppl. info). As for CoPc there are also bonds between the pyrrolic nitrogen atoms and the Co surface. The peak of the FePc N1s core level ($\Delta E = 0.84$ eV) only observed in XPS at low coverage is also strongly shifted, with a shift comparable to that found in CoPc (SI). These relatively large shifts for both N1 core levels in CoPc and FePc cannot be understood in terms of a site-specific screening effect due to image charge screening at the interface with typical values in the range of 0.1–0.4 eV.[30] The behavior of the nitrogen-Co interaction underlines the important role of the metal atom because the pyrrolic nitrogen is the binding element between the organic ring and the central metal atom. The role of the nitrogens is also highlighted in the magnetization density plot of FePc shown for the energetically favored ferromagnetic coupling ($J = 0.110$ eV) with the Co surface in Figure 5d, leading to a magnetic moment (3d orbitals) of 1.94 μ_B. The magnetization density distribution dominated by ferromagnetic coupling of the iron central atom changes into an antiferromagnetic coupling order located in the molecular plane and on the pyrrolic nitrogen atoms coordinating the iron atom. A second antiferromagnetic coupling is found at the ligand phenyl-ring side. A magnetic coupling to the surface mediated by nitrogens atoms was previously found for iron porphyrin molecules on Co.[31]

5. Conclusions

State-of-the-art DFT+U calculations in combination with UPS and XPS photoelectron spectroscopy as well as spin-resolved UPS measurements directly demonstrate the formation of new hybrid interface states (HIS), induced by chemisorption of CuPc, CoPc, and FePc at the Co surface. The correlation between ab initio calculations and experimental data unveils the crucial role of the partially occupied frontier d-orbitals of the central metal atom and their symmetry in the formation of metallic behavior with spin-polarized interface states at and near the Fermi level. Whereas FePc and CoPc have only weakly spin-polarized levels at E_F, CuPc shows strong spin-polarization directly at the Fermi level. On the other hand, salient differences in the interaction of the central metal atom and the FM lead to a vanishing magnetic moment in case of CuPc and a strong ferromagnetic coupling in case of CoPc with a magnetic moment of 0.515 μ_B and FePc with a magnetic moment of 1.94 μ_B. The difference between CoPc and FePc on the one hand, and CuPc on the other, is the symmetry of the d-orbital(s) which mostly constitute the singly occupied molecular orbitals (SOMO) of the open shell MPc's and are massively involved in the hybridization: Whereas CoPc and FePc have strong contributions of orbitals perpendicular to the molecular plane which favors π-type interaction with the d-orbitals of the substrate (bridged position), CuPc has only a weak interaction through an in-plane d-orbital (d_{x2-y2}). All this demonstrates that by changing the transition metal atom in this organo-metallic molecule the magnetic behaviour and, in particular, the spin-polarization at the Fermi level itself can be modified successfully in the first monolayer of such inorganic/organic hybrid structures by hybrid interface states. In a second step, these spin polarized HIS can couple to the bulk states of the following layers of an appropriate second organic molecule by a tunneling process which then can conserve the spin polarization. Thus, tuning spin-selectively the DOS at E_F by chemisorption induced HIS creates very advantageous conditions for subsequent spin injection into the next organic layers if they consist of appropriately chosen molecules. In future studies it has to be investigated whether the symmetry of the involved metal d-orbitals of the metal–organic OSC plays this dominant role not only in phthalocyanines but also in other metal–organics. Such a finding would consequently be highly important for spintronic applications of organic semiconductors as it provides an appealing way of engineering spin-selective injection channels at the OSC-FM interface.

6. Experimental Section

All experiments were performed in-situ in an ultrahigh vacuum system with a base pressure below $5 \cdot 10^{-10}$ mbar. Spin-integrated spectra were recorded with a Specs Phoibos 150 analyzer, spin-resolved data with a Scienta R4000 equipped with a Mott detector. The Co thin films were epitaxially grown on a Cu(001) single crystal. The Cu substrates were prepared by repeated cycles of Ar-ion bombardment and subsequent annealing procedures to obtain an oxygen and carbon free substrate. Subsequently the Co layer was deposited by using a commercial e-beam evaporator (Omicron EFM3) and a deposition rate of 0.05 nm min^{-1}. The layer thickness of the Co substrate was 10 ML. The MPc thin films were deposited in situ on the freshly prepared Co-film. The deposition of the organic films and the Co were monitored with an integrated quartz crystal microbalance calibrated with scanning force microscopy measurements. The deposition rates for the MPc were determined to be around 0.4 nm min^{-1}. Because of the required high purity of the interface, the chemical purity of all layers was checked by means of X-ray photoemission spectroscopy (XPS). To avoid any oxidation of the Co substrate the XPS analysis was additionally supported by checking the absence of any oxygen typical structures which would be visible already in a very early stage of surface oxidation. For the multilayer films a homogeneous growth was checked by monitoring the relationship of the core level intensity for the Co $2p_{3/2}$ signal of the substrate and the carbon C1s signal of the OSC.

Our calculations are based on the density-functional theory +U (DFT+U) approach, in which strong Coulomb interactions occurring within the open 3d-shell of the TM ion are captured by the supplemented Coulomb and exchange constants U and J. In the present calculations U and J were taken to be 4 eV and 1 eV, respectively. These values were shown to provide the correct spin state for free and absorbed metalloporphyrins, in contrast to standard DFT calculations in the commonly used generalized gradient approximation (GGA).[12,33]

Here we have used the VASP full-potential plane-wave code, in which pseudo-potentials together within the projector augmented wave method are used.[34,35] A kinetic energy cut-off of 400 eV was employed for the plane waves. For the DFT-GGA exchange-correlation functional we used the Perdew-Wang parameterization.[36] The metallic surface was modeled through three atomic layers Co (adopting the fcc Co lattice parameter of 3.61 Å). We performed full geometric optimizations of the phthalocyanine molecules, of their distance to and positions on the surface, together with a full relaxation of the top Co layer. For the reciprocal space sampling we used $2 \times 2 \times 2$ Monkhorst-Pack *k*-points. For comparability between the theoretical results and the experimental SP-UPS data, all calculated LDOS were stretched in energy by 1.4. This scaling factor was determined by comparing the energy scale of the LDOS data for the single molecules with the one found for experimental photoelectron gas phase spectra of the MPs molecules.

Supporting Information

Supporting Information is available from the Wiley Online Library or from the author.

Acknowledgements

Fruitful discussions with G. Schmidt, Halle, are gratefully acknowledged. This work has partly been supported by the Swedish-Indian Research Links Programme, the C. Tryggers Foundation, and the Swedish National Infrastructure for Computing (SNIC). This article was amended on March 7, 2012 to correct the author names and academic titles, which were incorrect in the version originally published online. Several typographical errors were also corrected.

Received: September 26, 2011
Revised: November 22, 2011
Published online: December 21, 2011

[1] V. Dediu, M. Mugia, F. Matacotta, C. Taliani, S. Barbanera, *Solid State Commun.* **2002**, *122*, 181–184.
[2] V. Dediu, L. E. Hueso, I. Bergenti, C. Taliani, *Nat. Mater.* **2009**, *8*, 707–716.
[3] Z. H. Xiong, D. Wu, Z. V. Vardeny, J. Shi, *Nature* **2004**, *427*, 821–824.
[4] L. Schulz, L. Nuccio, M. Willis, P. Desai, P. Shakya, T. Kreouzis, V. K. Malik, C. Bernhard, F. L. Pratt, N. A. Morley, A. Suter, G. J. Nieuwenhuys, T. Prokscha, E. Morenzoni, W. P. Gillin, A. J. Drew, *Nat. Mater.* **2011**, *10*, 39–44.
[5] K. V. Raman, J. Chang, J. S. Moodera, *Org. Electron.* **2011**, *12*, 1275–1278.
[6] P. A. Bobbert, W. Wagemans, F. W. A. Bloom, B. Koopmans, M. Wohlgenannt, *Phys. Rev. Lett.* **2009**, *102*, 156604.
[7] V. I. Krinichnyi, *Synth. Met.* **2000**, *108*, 173–222.
[8] J. F. Ren, J. Y. Fu, D. S. Liu, L. M. Mei, S. J. Xie, *Synth. Met.* **2005**, *155*, 611–614.
[9] S. Pramanik, C.-G. Stefanita, S. Patibandla, S. Bandyopadhyay, K. Garre, N. Harth, M. Cahay, *Nat. Nanotech.* **2007**, *2*, 216–219.
[10] G. Schmidt, D. Ferrand, L. W. Molenkamp, *Phys. Rev. B* **2000**, *62*, R4790.
[11] C. Barraud, P. Seneor, R. Mattana, S. Fusil, K. Bouzehouane, C. Deranlot, P. Graziosi, L. Hueso, I. Bergenti, V. Dediu, F. Petroff, A. Fert, *Nat. Phys.* **2010**, *6*, 615–620.
[12] Md. E. Ali, B. Sanyal, P. M. Oppeneer, *J. Phys. Chem. C* **2009**, *113*, 14381–14383.
[13] S. Sanvito, *Nat. Phys.* **2010**, *6*, 562–564.
[14] Y. Zhan, E. Holmström, R. Lizárraga, O. Eriksson, X. Liu, F. Li, E. Carlegrim, S. Stafström, M. Fahlman, *Adv. Mater.* **2010**, *22*, 1626–1630.
[15] S. Javaid, M. Bowen, S. Boukari, L. Joly, J.-B. Beaufrand, X. Chen, Y. J. Dappe, F. Scheurer, J.-P. Kappler, J. Arabski, W. Wulfhekel, M. Alouani, E. Beaurepaire, *Phys. Rev. Lett.* **2010**, *105*, 077201.
[16] M. Cinchetti, K. Heimer, J.-P. Wüstenberg, O. Andreyev, M. Bauer, S. Lach, Ch. Ziegler, Y. Gao, M. Aeschlimann, *Nat. Mater.* **2009**, *8*, 115–119.
[17] C. Iacovita, M. V. Rastei, B. W. Heinrich, T. Brumme, J. Kortus, L. Limot, J. P. Bucher, *Phys. Rev. Lett.* **2008**, *101*, 116602.
[18] J. Brede, N. Atodiresei, S. Kuck, P. Lazić, V. Caciuc, Y. Morikawa, G. Hoffmann, S. Blügel, R. Wiesendanger, *Phys. Rev. Lett.* **2010**, *105*, 047204.
[19] N. Marom, O. Hod, G. E. Scuseria, L. Kronik, *J. Chem. Phys.* **2008**, *128*, 164107.
[20] N. Marom, L. Kronik, *Appl. Phys. A* **2009**, *95*, 165–172.
[21] B. Bialek, I. Gee Kim, J. I. Lee, *Thin Solid Films* **2006**, *513*, 110–113.
[22] C. C. Leznoff, A. B. Lever, *Phthalocyanines: Properties and Applications*. Wiley & Sons, New York **1993**.
[23] C. M. Schneider, J. J. de Miguel, P. Bressler, P. Schuster, R. Miranda, J. Kirschner, *J. Electron. Spectr. Rel. Phenomena* **1990**, *51*, 263–274.
[24] A. B. Schmidt, M. Pickel, T. Allmers, M. Budke, J. Braun, M. Weinelt, M. Donath, *J. Phys. D: Appl. Phys.* **2008**, *41*, 164003.
[25] L. Gonzales, R. Miranda, M. Salmeron, J. A. Verges, F. Yndurain, *Phys. Rev. B* **1981**, *24*, 3245–3254.
[26] M. Vogel, F. Schmitt, J. Sauther, B. Baumann, A. Altenhof, S. Lach, Ch. Ziegler, *Anal. Bioanal. Chem.* **2011**, *400*, 673–678.
[27] S. Braun, W. R. Salaneck, M. Fahlman, *Adv. Mat.* **2009**, *21*, 1450–1472.
[28] C. Shen, A. Kahn, *Org. Electron.* **2001**, *2*, 89–95.
[29] K. Miyamoto, K. Iori, K. Sakamoto, H. Narita, A. Kimura, M. Taniguchi, S. Qiao, K. Hasegawa, K. Shimada, H. Namatame, S. Blügel, *New J. Phys.* **2008**, *10*, 125032.
[30] G. Dufour, C. Poncey, F. Rochet, H. Roulet, M. Sacchi, M. De Santis, M. De Crescenzi, *Surf. Sci.* **1994**, *319*, 251–266.
[31] H. Wende, M. Bernien, J. Luo, C. Sorg, N. Ponpandian, J. Kurde, J. Miguel, M. Piantek, X. Xu, Ph. Eckhold, W. Kuch, K. Baberschke, P. M. Panchmatia, B. Sanyal, P. M. Oppeneer, O. Eriksson, *Nat. Mater.* **2007**, *6*, 516–520.
[32] A. Ruocco, F. Evangelista, R. Gotter, A. Attili, G. Stefani, *J. Phys. Chem. C* **2008**, *112*, 2016–2025.
[33] P. M. Oppeneer, P. M. Panchmatia, B. Sanyal, O. Eriksson, Md. E. Ali, *Prog. Surf. Sci.* **2009**, *84*, 18–29.
[34] G. Kresse, J. Furthmüller, *Phys. Rev. B* **1996**, *54*, 11169–11186.
[35] P. E. Blöchl, *Phys. Rev. B* **1994**, *50*, 17953–17979.
[36] J. P. Perdew, J. Wang, *Phys. Rev. B* **1992**, *45*, 13244–13249.